Petroleum Science 20 (2023) 3085–3099

Contents lists available at ScienceDirect

Petroleum Science

journal homepage: www.keaipublishing.com/en/journals/petroleum-science

Original Paper

Hydraulic modeling and optimization of jet mill bit considering the characteristics of depressurization and cuttings cleaning

Tong Cao [a], Xu-Yue Chen [b, *], Kai-An Yu [c], Lin Tang [a]

[a] School of Mechatronic Engineering, Xi'an Technological University, Xi'an, Shaanxi, 710021, China
[b] MOE Key Laboratory of Petroleum Engineering, China University of Petroleum, Beijing, 102249, China
[c] College of Mechanical and Transportation Engineering, China University of Petroleum, Beijing, 102249, China

ARTICLE INFO

Article history:
Received 5 October 2022
Received in revised form
25 December 2022
Accepted 5 April 2023
Available online 11 April 2023

Edited by Jia-Jia Fei

Keywords:
Jet mill bit
Hydraulic depressurization model
Hydraulic cuttings cleaning model
Parametric study
Hydraulic optimization

ABSTRACT

A jet mill bit (JMB) is proposed to increase the drilling efficiency and safety of horizontal wells, which has the hydraulic characteristics of depressurization and cuttings cleaning. This paper fills the gap in the hydraulic study of the JMB by focusing on the hydraulic modeling and optimization of the JMB and considering these two hydraulic characteristics. First, the hydraulic depressurization model and the hydraulic cuttings cleaning model of the JMB are developed respectively. In the models, the pressure ratio and efficiency are chosen as the evaluation parameters of the depressurization capacity of the JMB, and the jet hydraulic power and jet impact force are chosen as the evaluation parameters of cuttings cleaning capacity of the JMB. Second, based on the hydraulic models, the effects of model parameters [friction loss coefficient, target inclination angle, rate of penetration (ROP), flow ratio, and well depth] on the hydraulic performance of the JMB are investigated. The results show that an increase in the friction loss coefficient and target inclination angle cause a significant reduction in the hydraulic depressurization capacity, and the effect of ROP is negligible. The flow ratio is positively related to the hydraulic cuttings cleaning capacity, and the well depth determines the maximum hydraulic cuttings cleaning capacity. Finally, by combining the hydraulic depressurization model and hydraulic cuttings cleaning model, an optimization method of JMB hydraulics is proposed to simultaneously maximize the jet depressurization capacity and the cuttings cleaning capacity. According to the drilling parameters given, the optimal values of the drilling fluid flow rate, backward nozzle diameter, forward nozzle diameter, and throat diameter can be determined. Moreover, a case study is conducted to verify the effectiveness of the optimization method.

1. Introduction

With the development of unconventional oil and gas resources, the number of horizontal wells is increasing rapidly, and the question of how to increase the drilling efficiency and safety of horizontal wells has become a pressing concern (Adesina et al., 2011; Chen et al., 2021a, 2021b; Tang et al., 2019; Wu et al., 2020). In response to this concern, a unique bit referred to as the jet mill bit (JMB) with complex internal flow channels is proposed, which can improve rate of penetration (ROP) and cuttings transportation efficiency via the jet depressurization effect and jet cuttings crushing effect (Cao et al., 2019; Chen et al., 2016a, 2020; Chen and Gao, 2016; Chen et al., 2016b). Due to the addition of complex internal flow channels, the drilling fluid entering the JMB is split into two streams: part of the drilling fluid flows into backward nozzles to clean cuttings and cool the cutters, and another part of the drilling fluid flows into forward nozzles to generate the low-pressure zone to draw the bottom hole drilling fluid and reduce bottom hole pressure. Therefore, the JMB has not only cuttings cleaning characteristic but also depressurization characteristic, and both characteristics should be considered in the hydraulics of the JMB.

As shown in Fig. 1, the depressurization capacity of the JMB is realized by a jet negative pressure suction device, which has a working principle similar to that of a jet pump. Therefore, a hydraulic study of the depressurization characteristic of a JMB can be

* Corresponding author.
E-mail address: chenxuyue2011@163.com (X.-Y. Chen).

https://doi.org/10.1016/j.petsci.2023.04.007

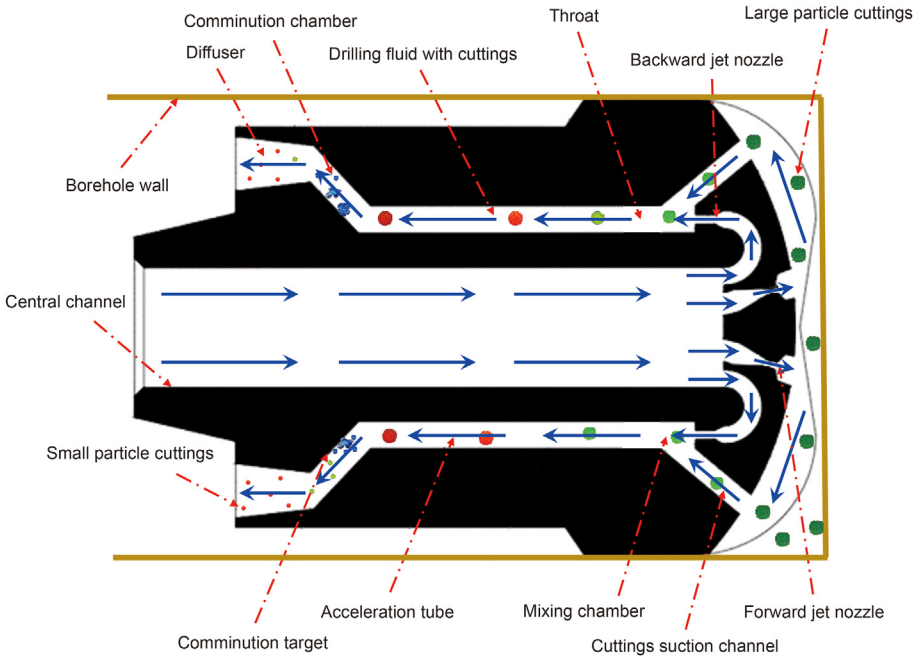

Fig. 1. Structure diagram of JMB.

based on the jet pump theory. The jet pump, which was first used by James Thompson in 1852, has three main components: nozzle, throat, and diffuser. Rankine (1871) introduced the mathematical theory of jet pumps based on momentum theory in 1870; afterward, many researchers published a number of papers and developed jet pump technology. Gosline and O'Brien (1934) carried out theoretical and experimental studies on liquid jet pumps and established a basic characteristic equation that is considered standard reference work. Cunningham (1957) conducted an experimental program of eight jet pumps with different nozzle-to-throat area ratios and established the basic characteristic equation of the jet pump, which introduced dimensionless ratios and friction coefficients. Kermit (1980) introduced the application of a jet pump in oil recovery and proposed a calculation method of the pressure ratio based on the work of Gosline. Grupping et al. (1988) established the basic characteristic equation of a jet pump when the power fluid and suction fluid have different densities, introduced a dimensional mass flow ratio, and provided a set of design and analysis methods for a jet pump for oil recovery. Wang et al. (2004a) derived a calculation formula for the efficiency of a jet pump and developed an optimal parameter model to maximize the efficiency. The results showed that the optimal area ratio was 0.28 when the density ratio was 1, and the friction loss coefficients were given by Kermit (1980).

Except for the depressurization capacity, the cuttings cleaning capacity of the JMB is the same as that of the common bit. The hydraulics of the bit determine the ability of the drilling fluid to effectively transport cuttings from the bottom hole and eliminate bit balling and are viewed as the primary tool to improve the ROP and reduce the drilling cost. Therefore, optimization of bit hydraulics has been a popular topic for several decades. Speer (1959) first found that an increase in mud pump power directly improves the hydraulic performance of the bit, but the ROP will not always increase with increasing mud pump power. Later, it was recognized that the efficient utilization of mud pump power is also important for improving ROP because the hydraulics of the bit have a more direct influence on bit performance. Kendall and Goins (1960) developed methods to maximize the hydraulic quantities of bit, including hydraulic horsepower, jet impact force, and jet velocity, while the pump pressure, well depth and pressure loss in drilling fluid circulation system were considered in the methods. McLean (1965) found through experiments that the bit performance is best when the bit jet impact force is maximum because the velocity of the drilling fluid across the bottom hole is also maximum at that time. More recently, bit structure parameters (junk slot area, face volume, etc.) and non-circle nozzles were used to improve the hydraulic performance of the bit (Schnuriger et al., 2017; Wells et al., 2008).

Although a number of models have been developed for the hydraulic performance of jet pumps and common bits, there is no available model or method for optimizing JMB hydraulics in terms of depressurization capacity and cuttings cleaning capacity; therefore, this paper seeks to fill this gap. In this paper, a hydraulic depressurization model of the JMB is developed based on the theory of the jet pump, and a hydraulic cuttings cleaning model of the JMB is developed based on the theory of jet hydraulic power and jet impact force to evaluate and analyze the depressurization capacity and cuttings cleaning capacity of the JMB. Furthermore, the relation between these two hydraulic models is developed, the optimization method of JMB hydraulics is proposed to simultaneously maximize the depressurization capacity and the cuttings cleaning capacity, and the optimization procedure is illustrated with a case study.

2. Principle of JMB

Based on the principle of the jet pump and jet crushing (Beithou and Aybar, 2001; Liu et al., 2019; Wang et al., 2021; Zhu and Liu, 2015), the JMB is combined with jet negative pressure suction devices and jet cuttings crushing devices to achieve the suction of bottom hole drilling fluid and the secondary crushing of cuttings, as shown in Fig. 1. The jet negative pressure suction device is composed of a backward nozzle, cuttings suction channel, mixing chamber, and acceleration tube. The jet cuttings crushing device is composed of an acceleration tube, comminution chamber, comminution target, and diffuser.

The action mechanism of the jet negative pressure suction device is as follows: when the high-pressure drilling fluid enters the central channel inside the JMB, it splits into two streams at the intersections of the forward and backward nozzles. Drilling fluid through the forward nozzle cleans the bottom hole and cools the cutters, preventing the cutters from being muddy and overheated. Drilling fluid through the backward nozzle generates a low-pressure zone at the outlet of the backward nozzle. As a result of the pressure difference, the bottom hole drilling fluid is suctioned to enter the cuttings suction channel, thereby decreasing the bottom hole pressure and reducing the cuttings hold-down effect, both of which are advantageous for enhancing the ROP.

The action mechanism of the jet crushing cuttings device is as follows: the bottom hole drilling fluid with cuttings is suctioned to enter the mixing chamber, where it mixes and exchanges energy with high-speed drilling fluid from the backward nozzle; the cuttings is dragged by the high-speed drilling fluid to accelerate along the acceleration tube; then high-velocity cuttings violently collides with the comminution target in the comminution chamber, and the enormous shock stress waves generated at the moment of collision can destroy the bond within the cuttings particle, resulting in the secondary crushing of cuttings. This is advantageous for cuttings transportation efficiency and fundamentally eliminating the cuttings bed in horizontal wells.

3. Hydraulic depressurization modeling of JMB

3.1. Hydraulic characteristic parameters of JMB

The hydraulic depressurization structure of JMB is shown in Fig. 2. p_1 is the pressure of drilling fluid in central channel inside JMB, Pa; q_1 is the volume flow of power drilling fluid (through backward nozzles), m^3/s; ρ_1 is the density of drilling fluid in central channel inside JMB, kg/m^3; q_2 is the volume flow of drilling fluid through forward nozzles, m^3/s; p_3 is the pressure of suction drilling fluid, Pa; q_3 is the volume flow of suction drilling fluid, m^3/s; ρ_3 is the density of suction drilling fluid (drilling fluid with cuttings), kg/m^3; p_4 is the outlet pressure of diffuser, Pa; q_4 is the volume flow of mixed drilling fluid, m^3/s; ρ_4 is the density of mixed drilling fluid, kg/m^3; A_u is the outlet area of backward nozzle, m^2; A_t is the cross-sectional area of throat, m^2; A_s is the cross-sectional area of the annual between backward nozzle and throat, m^2; and θ is the angle between comminution target and central line of throat, rad.

To analyze and evaluate the hydraulic depressurization capacity of the JMB, it is necessary to develop a hydraulic depressurization model. First, the dimensional characteristic parameters are given as follows.

3.1.1. Dimensionless pressure ratio P

The dimensionless pressure ratio P is defined as the ratio between the pressure increment of the suction drilling fluid and the pressure decrement of the power drilling fluid and can be given as

$$P=\frac{p_4-p_3}{p_1-p_4} \tag{1}$$

The larger the dimensionless pressure ratio P, the stronger the suction effect of the JMB on the bottom hole drilling fluid.

3.1.2. Dimensionless flow ratio M

The dimensionless flow ratio M is defined as the ratio between the volume flow of the suction drilling fluid and power drilling fluid, which can be given as

$$M=\frac{q_3}{q_1}=\frac{d_d^2}{d_u^2} \tag{2}$$

where d_u is the diameter of the backward nozzle, m; and d_d is the diameter of the forward nozzle, m.

3.1.3. Dimensionless area ratio R

The dimensionless area ratio R is defined as the area ratio between the outlet area of the backward nozzle and the cross-sectional area of the throat, which can be given as

$$R=\frac{A_u}{A_t} \tag{3}$$

When the wall thickness of the backward nozzle is ignored, Eq. (3) can be written as

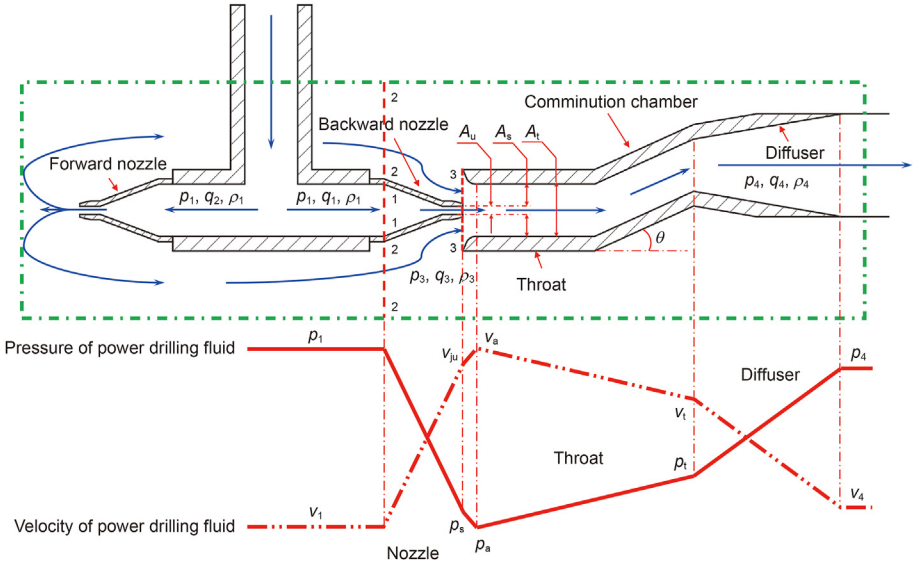

Fig. 2. Schematic diagram of hydraulic depressurization structure of JMB.

$$R=\frac{{d_u}^2}{{d_t}^2} \tag{4}$$

where d_t is the diameter of the throat, m.

Accordingly, the flow velocity can be written as

$$v_{ju}=\frac{q_1}{A_u} \tag{5}$$

$$v_s=\frac{q_3}{A_s}=\frac{Mq_1}{\frac{A_u}{R}-A_u}=\frac{MRv_{ju}}{1-R} \tag{6}$$

$$v_t=\frac{q_4}{A_t}=\frac{q_1+Mq_1}{\frac{A_u}{R}}=(1+M)Rv_{ju} \tag{7}$$

where v_{ju} is the flow velocity of drilling fluid passing through the backward nozzle, m/s; v_s is the flow velocity of drilling fluid passing through the inlet of the throat, m/s; and v_t is the flow velocity of mixed drilling fluid passing through the throat, m/s.

3.1.4. Dimensional density ratio ρ

The dimensional density ratio ρ is defined as the density ratio between the suction drilling fluid and power drilling fluid and can be given as

$$\rho=\frac{\rho_3}{\rho_1} \tag{8}$$

After mixing the suction drilling fluid and power drilling fluid in the mixing chamber, the density of the mixed drilling fluid ρ_4 can be written as

$$\rho_4=\frac{\rho_1q_1+\rho_3q_3}{q_1+q_3}=\frac{1+\rho M}{1+M}\rho_1 \tag{9}$$

It is assumed that cuttings generated during drilling are fully and quickly mixed with drilling fluid, and the effect of cuttings volume is negligible. Then, the relationship between the density of suction drilling fluid and ROP can be written as

$$\rho_3=\frac{\frac{R_{op}}{3600}\pi\left(\frac{d_w}{2}\right)^2\rho_r}{q_3}+\rho_1=\frac{R_{op}\pi{d_w}^2\rho_r}{14400q_3}+\rho_1 \tag{10}$$

where R_{op} is the rate of penetration, m/h; d_w is the diameter of the wellbore, m; and ρ_r is the density of rock, kg/m^3.

Substituting Eq. (10) into Eq. (8), the density rate ρ can be written as

$$\rho=1+\frac{R_{op}\pi{d_w}^2\rho_r}{14400q_3\rho_1} \tag{11}$$

3.2. Derivation of the hydraulic depressurization characteristic equation of the JMB

In this section, a hydraulic depressurization characteristic equation is developed to complete the theoretical analysis of JMB hydraulics. Considering that the flow condition of drilling fluid in the internal structures of the JMB is quite complex, it is difficult to analyze the flow mechanism from a theoretical standpoint. Therefore, the model constructed in this section focuses only on the input and output characteristics of the JMB from an energy-work perspective. The following assumptions are provided to facilitate model derivation:

(1) The variation in the viscosity of the drilling fluid is ignored.
(2) The effect of the distance between the backward nozzle and throat is ignored.
(3) All drilling fluid from the bottom hole returns upward through the suction channel.
(4) In the mixing chamber, the power drilling fluid and suction drilling fluid are thoroughly mixed.
(5) All the hydraulic depressurization structures are the same and uniformly distributed on the JMB in circumferential direction.

The energy conservation equation of drilling fluid flowing through the JMB can be expressed as follows:

$$E_j=E_s+L_m+L_j+L_s+L_{td}+L_c \tag{12}$$

where E_j is the energy provided by power drilling fluid in unit time, W; E_s is the energy obtained by suction drilling fluid in unit time, W; L_m is the energy loss in unit time during mixing of suction drilling fluid and power drilling fluid in the throat, W; L_j is the energy loss in unit time when drilling fluid passes through nozzles, W; L_s is the energy loss in unit time when drilling fluid passes the cuttings suction channel, W; L_{td} is the energy loss in unit time when mixed drilling fluid passes through the throat and diffuser, W; L_c is the energy loss in unit time when mixed drilling fluid passes through the comminution chamber, W.

The energy provided by the power drilling fluid in unit time can be written as

$$E_j=q_1(p_1-p_4)+q_2(p_1-p_3) \tag{13}$$

The energy obtained by suction drilling fluid in unit time can be written as

$$E_s=q_3(p_4-p_3) \tag{14}$$

Based on the Lorenz mixed loss model (Kermit, 1980; Wang et al., 2004b; Winoto et al., 2000), the energy loss in unit time during the mixing of suction drilling fluid and power drilling fluid in the throat can be written as

$$L_m=\frac{1}{2}\left[\rho_1q_1(v_{ju}-v_t)^2+\rho_1q_2\left(v_{jd}-v_s\right)^2+\rho_3q_3(v_s-v_t)^2\right] \tag{15}$$

where v_{jd} is the velocity of drilling fluid passing through the forward nozzle, m/s.

The energy loss in unit time of drilling fluid passing through nozzles can be written as (Wang et al., 2004a)

$$L_j=L_{ju}+L_{jd}=\frac{1}{2}\left(\rho_1q_1K_{ju}v_{ju}^2+\rho_1q_2K_{jd}v_{jd}^2\right) \tag{16}$$

where L_{ju} is the energy loss in unit time of drilling fluid passing through the backward nozzles, W; L_{jd} is the energy loss in unit time of drilling fluid passing through the forward nozzles, W; K_{ju} is the friction loss coefficient of the backward nozzle; and K_{jd} is the friction loss coefficient of the forward nozzle.

The forward and backward nozzles are connected with the central channel; therefore, the velocities of drilling fluid passing through different nozzles are the same, which is shown in Eq. (17). The friction loss coefficient is proportional to the flow rate, which can be shown as

$$v_{ju} = v_{jd} \tag{17}$$

$$\frac{K_{jd}}{K_{ju}} = \frac{q_3}{q_1} = M \tag{18}$$

Substituting Eqs. (17) and (18) into Eq. (16), the following equation can be obtained.

$$L_j = \left(1 + M^2\right)\frac{1}{2}\rho_1 q_1 K_{ju} v_{ju}^2 \tag{19}$$

Combined with Eqs. (2) and (6) and Eq. (8), the energy loss in unit time when drilling fluid passes the cuttings suction channel can be written as

$$L_s = \frac{1}{2}\rho_3 q_3 K_s v_s^2 = \rho M\left(\frac{MR}{1-R}\right)^2\frac{1}{2}\rho_1 q_1 K_s v_{ju}^2 \tag{20}$$

where K_s is the friction loss coefficient of the annular channel of the throat inlet.

Combined with Eqs. (2) and (7), and Eq. (9), the energy loss in unit time when mixed drilling fluid passes through the throat and diffuser can be written as

$$\begin{aligned} L_{td} = L_t + L_d &= \frac{1}{2}\left(\rho_4 q_4 K_t v_t^2 + \rho_4 q_4 K_d v_t^2\right) = \frac{1}{2}\rho_4 q_4 K_{td} v_t^2 \\ &= (1+\rho M)(1+M)^2 R^2 \frac{1}{2}\rho_1 q_1 K_{td} v_{ju}^2 \end{aligned} \tag{21}$$

where L_t is the energy loss in unit time of mixed drilling fluid passing through the throat, W; L_d is the energy loss in unit time of mixed drilling fluid passing through the diffuser, W; K_t is the friction loss coefficient of the throat; K_d is the friction loss coefficient of the diffuser; and K_{td} is the sum of the friction loss coefficient of the throat and diffuser.

Combined with Eqs. (2) and (7) and Eq. (9), the energy loss in unit time when mixed drilling fluid passes the comminution chamber can be written as (Berger et al., 1983; Qi, 2017)

$$L_c = \frac{1}{2}\rho_4 q_4 \xi v_t^2 = (1+\rho M)(1+M)^2 R^2 \frac{1}{2}\rho_1 q_1 \xi v_{ju}^2 \tag{22}$$

$$\xi = 1.892\sin^2\left(\frac{\theta}{2}\right) + 4.094\sin^4\left(\frac{\theta}{2}\right) \tag{23}$$

where ξ is the local resistance coefficient; and θ is the inclination angle of the comminution target, rad.

Substituting Eq. (13)–(15) and Eq. (19)–(22) into Eq. (12), the energy conservation equation of the JMB can be written as

$$\begin{aligned} (1+M)(p_1 - p_4) = \frac{1}{2}\rho_1 v_{ju}^2 \Bigg[&\rho M\left(\frac{MR}{1-R}\right)^2 K_s + \\ &(1+\rho M)(1+M)^2 R^2 (K_{td} + \xi) + \left(1+M^2\right)K_{ju} + (1-R-MR)^2 + \\ &M\left(1-\frac{MR}{1-R}\right)^2 + \rho M\left(\frac{MR}{1-R} - R - MR\right)^2 \Bigg] \end{aligned} \tag{24}$$

As shown in Fig. 2, the outlet of the backward nozzle is set to Section 3-3, the inlet of the backward nozzle is set to Section 1-1, and the drilling fluid suction port is set to Section 2-2. Based on Bernoulli's principle, the energy conservation equation of power drilling fluid flowing from Section 1-1 to Section 3-3 and the energy conservation equation of suction drilling fluid flowing from Section 2-2 to Section 3-3 can be built. Since the kinetic energy of the power drilling fluid in Section 1-1 and suction drilling fluid in Section 2-2 are negligible, the following energy conservation equations can be obtained:

$$p_1 = p_s + \frac{1}{2}(1+K_{ju})\rho_1 v_{ju}^2 \tag{25}$$

$$p_3 = p_s + \frac{1}{2}(1+K_s)\rho_3 v_s^2 \tag{26}$$

Eq. (25) minus Eq. (26) to obtain

$$p_1 - p_3 = \frac{1}{2}(1+K_{ju})\rho_1 v_{ju}^2 - \frac{1}{2}(1+K_s)\rho_3 v_s^2 \tag{27}$$

Substituting Eqs. (6) and (8) into Eq. (27), the following equation can be obtained:

$$\frac{\rho_1 v_{ju}^2}{2} = \frac{p_1 - p_3}{1 + K_{ju} - (1+K_s)\rho\left(\frac{MR}{1-R}\right)^2} \tag{28}$$

Substituting Eq. (28) into Eq. (24), the following equation can be obtained:

$$\begin{aligned} (1+M)(p_1 - p_4) = \frac{p_1 - p_3}{1 + K_{ju} - (1+K_s)\rho\left(\frac{MR}{1-R}\right)^2} \Bigg[&\left(1+M^2\right) \\ &K_{ju} + \rho M\left(\frac{MR}{1-R}\right)^2 K_s + (1+\rho M)(1+M)^2 R^2 \\ &(K_{td} + \xi) + (1-R-MR)^2 + M\left(1-\frac{MR}{1-R}\right)^2 + \\ &\rho M\left(\frac{MR}{1-R} - R - MR\right)^2 \Bigg] \end{aligned} \tag{29}$$

For convenience, let

$$\lambda = \frac{\left(1+M^2\right)K_{ju} + \rho M\left(\frac{MR}{1-R}\right)^2 K_s + (1+\rho M)(1+M)^2 R^2 (K_{td}+\xi) + (1-R-MR)^2 + M\left(1-\frac{MR}{1-R}\right)^2 + \rho M\left(\frac{MR}{1-R} - R - MR\right)^2}{(1+K_{ju}) - (1+K_s)\rho\left(\frac{MR}{1-R}\right)^2} \tag{30}$$

Substituting Eq. (30) into Eq. (29), the following equation can be obtained:

$$(1+M) = \frac{p_1 - p_3}{p_1 - p_4}\lambda = (1+P)\lambda \tag{31}$$

From Eq. (31), the dimensionless pressure ratio P can be obtained as

$$P = \frac{1+M-\lambda}{\lambda} \tag{32}$$

The work efficiency E of the JMB is defined as the ratio between the energy increase of the suction drilling fluid and the energy decrease of the power drilling fluid and can be written as

$$E = \frac{E_s}{E_j} = \frac{MP}{1+M(1+P)} = \frac{M^2 - M\lambda + M}{M^2 + \lambda + M} \tag{33}$$

Eqs. (32) and (33) are the hydraulic depressurization

characteristic equations of the JMB, which can be used to analyze and evaluate the hydraulic depressurization capacity of the JMB.

3.3. Hydraulic characteristic curves of JMB

Based on Eqs. (32) and (33), the dimensionless pressure ratio P and work efficiency E can be expressed in the following functional form:

$$P = f_{\mathrm{P}}(M, \rho, R, K_{\mathrm{ju}}, K_{\mathrm{s}}, K_{\mathrm{td}}, \xi) \tag{34}$$

$$E = f_{\mathrm{E}}(M, \rho, R, K_{\mathrm{ju}}, K_{\mathrm{s}}, K_{\mathrm{td}}, \xi) \tag{35}$$

where the dimensionless area ratio R, friction loss coefficients (K_{ju}, K_{s}, K_{td}), and local resistance coefficient ξ depend on the internal structures and surface quality of the JMB, which are determined after the JMB is designed and machined. The density ratio ρ depends on the drilling fluid density and ROP, which varies during drilling. The flow rate M is controlled by the diameters of the forward and backward nozzles. The curves of P versus M and E versus M are called the hydraulic characteristic curves of the JMB, which are depicted in Fig. 3 using the parameter values from Table 1.

From Fig. 3, the following can be observed:

(1) The curves of E versus M are arched, and there is an efficiency peak.
(2) The curves of P versus M are on a downward trend, which indicates that the increment of suction drilling fluid can reduce the pressurization effect of JMB.
(3) The value of the area ratio R affects the efficiency peak and the working range of M. With the decrement of R, the changing trend of the maximum efficiencies of the E-M curves is arched, and the working range of M expands.

From Fig. 3, it is known that the area ratio R has an effect on the highest efficiency of the E-M curve. Therefore, the highest efficiency of the E-M curve with an area ratio is referred to as the local optimal efficiency E_{lopt}, and the corresponding R and P are referred to as the local optimal area ratio M_{lopt} and local optimal pressure ratio P_{lopt}, respectively. There is a maximum in the different E_{lopt} values, which is referred to as the global optimal efficiency E_{opt}, and the corresponding M and P are referred to as the global optimal flow ratio M_{opt} and global optimal pressure ratio P_{opt}. By calculating the pressure ratio P and efficiency E at different area ratios R, Figs. 4 and 5 can be obtained.

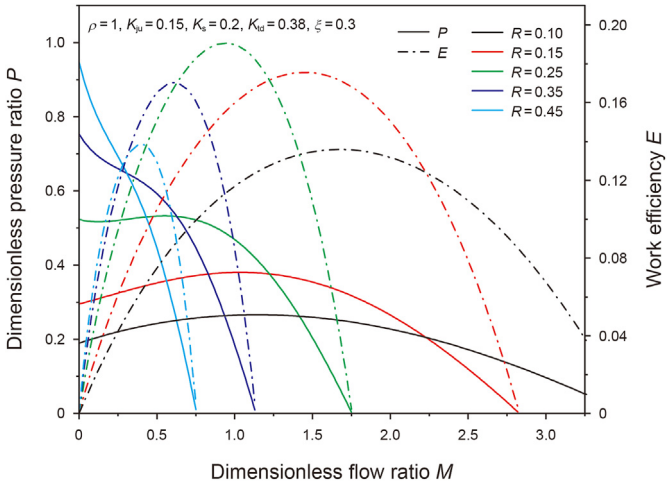

Fig. 3. Hydraulic characteristic curves of JMB.

Table 1
Parameter values of hydraulic model.

Parameter	ρ	K_{ju}	K_{s}	K_{td}	θ	ξ
Value	1	0.15	0.2	0.38	0.69	0.3

Note: the values of friction loss coefficients refer to typical values provided by Kermit and Winoto (Kermit, 1980; Winoto et al., 2000).

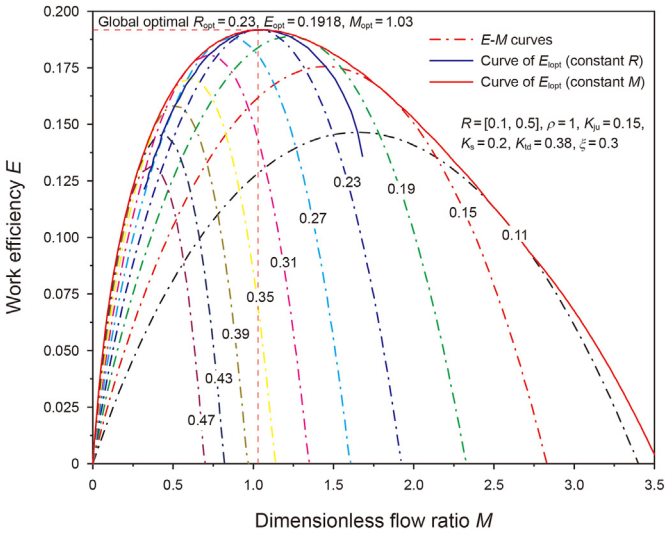

Fig. 4. Efficiency curves of JMB with different area ratios.

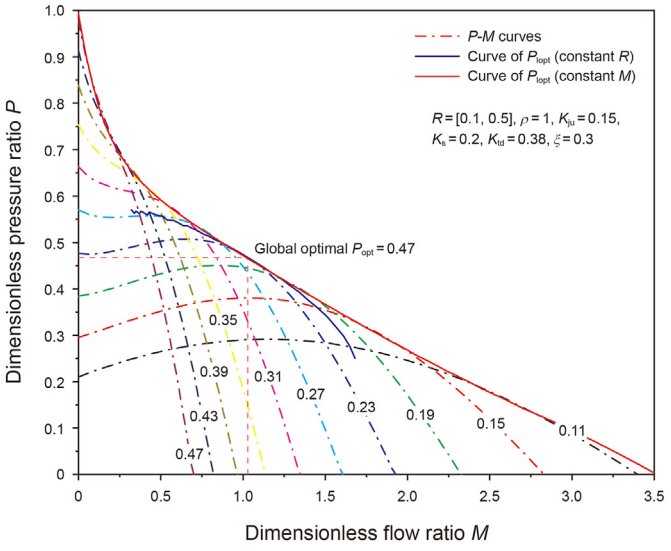

Fig. 5. Pressure ratio curves of JMB with different area ratios.

The curve of P_{lopt} (constant R) is the outer envelope of the E-M curves with different area ratios R, and the curve of P_{lopt} (constant M) is a line of the highest points of the E-M curves with different area ratios R. Observing these two curves reveals that P_{lopt} (constant R) is less than P_{lopt} (constant M) and that only at the global optimal point are they equal. The M corresponding to P_{lopt} is mostly in the range of 0.32–1.68, which is the high-efficiency flow ratio range of the JMB.

3.4. Parametric study of hydraulic depressurization capacity of JMB

In this section, a parametric study is conducted to investigate the effect mechanism of different parameters on the hydraulic depressurization capacity of the JMB.

3.4.1. Effect of friction loss coefficient

The greater the friction loss coefficient, the greater the energy loss of the drilling fluid. Figs. 6–8 illustrate the hydraulic characteristic curves for three friction loss coefficients. As the friction loss coefficients grow, it can be observed that the pressure ratio P and efficiency E of the JMB decline. In comparison to K_s and K_{td}, K_{ju} has a more significant negative effect on the hydraulic depressurization capacity of the JMB. When K_{ju} is 0.30, the maximum working efficiency is only 0.16, therefore K_{ju} should be controlled at a low level to obtain a high working efficiency.

3.4.2. Effect of target inclination angle

Fig. 9 depicts the hydraulic curves at different target inclination angles. The comminution target increases the energy loss of the drilling fluid and decreases the dimensionless pressure ratio and work efficiency of the JMB because the target impedes the flow of the drilling fluid. The greater the target inclination angle, the lower the hydraulic depressurization capacity of JMB.

When it is greater than 40°, the inclination angle θ has a significant negative influence on the hydraulic depressurization capacity of the JMB. To improve the hydraulic depressurization capacity of the JMB, the inclination angle should be controlled to be as small as possible. However, to improve the hydraulic cuttings crushing capacity of the JMB, the inclination angle should be controlled to be as large as possible. In light of this, the optimization of the inclination angle should strike a compromise between the hydraulic depressurization capacity and the hydraulic cuttings crushing capacity.

3.4.3. Effect of density ratio/ROP

From Eq. (11), it can be seen that the density ratio ρ is related to R_{op}, d_w, ρ_r, q_3, and ρ_1, and only R_{op} is the controllable parameter during drilling. Therefore, the effects of the density ratio/ROP on the hydraulic depressurization capacity of the JMB are investigated in this section, and the simulation results are shown in Figs. 10 and 11.

From Fig. 10, it can be seen that the hydraulic depressurization capacity decreases as the density ratio increases, because the increasing density ratio increases the energy loss of drilling fluid and the difficulty of suctioning drilling fluid. When ρ is 2, the local maximum efficiency is only 0.12, which indicates that the density ratio should be controlled at a low level.

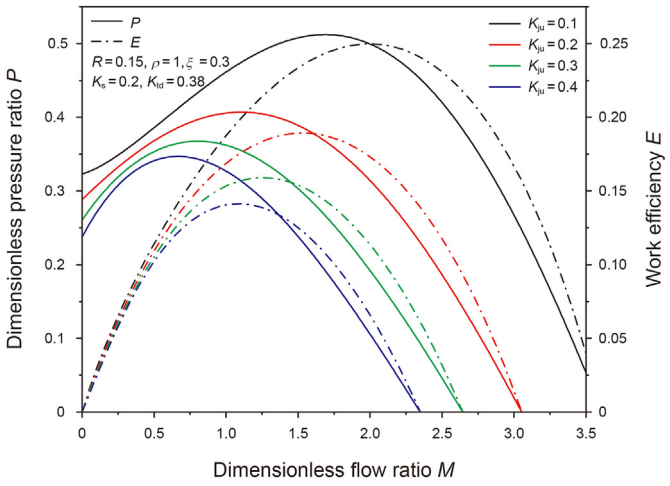

Fig. 6. Hydraulic characteristic curves at different K_{ju} values.

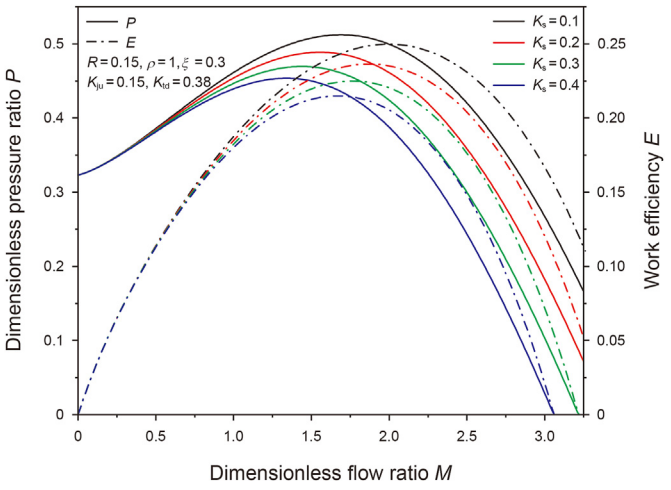

Fig. 7. Hydraulic characteristic curves at different K_s values.

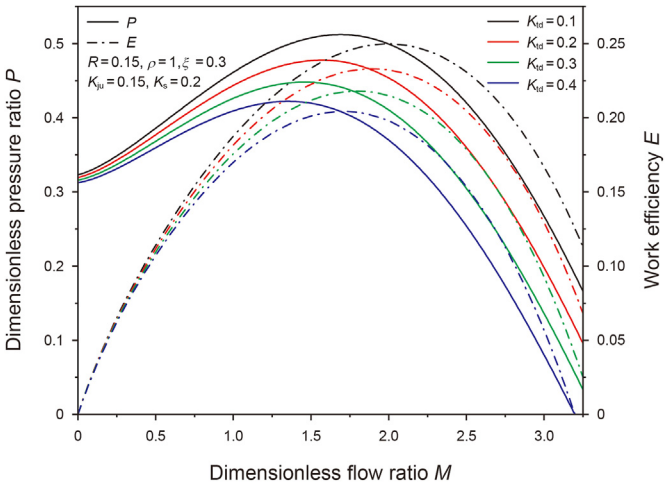

Fig. 8. Hydraulic characteristic curves at different K_{td} values.

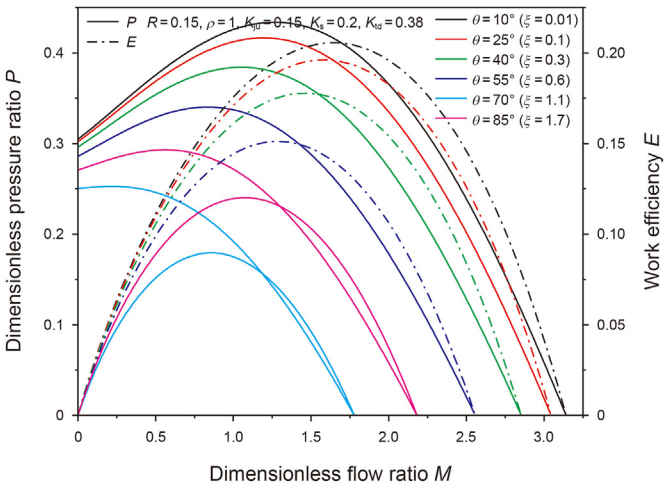

Fig. 9. Hydraulic characteristic curves at different target inclination angles θ

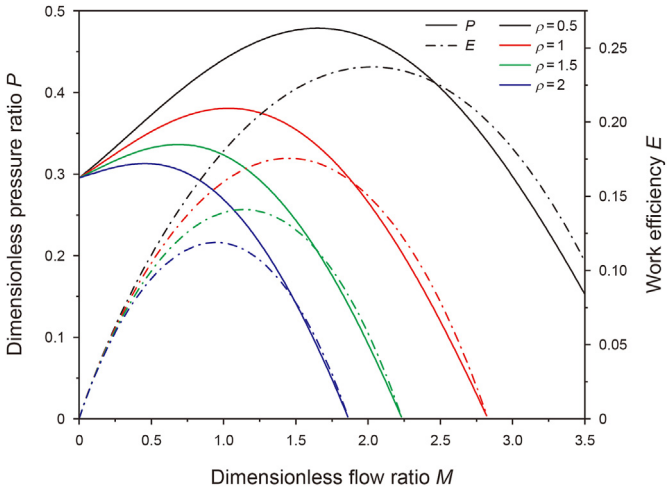

Fig. 10. Hydraulic characteristic curves at different density ratios ρ

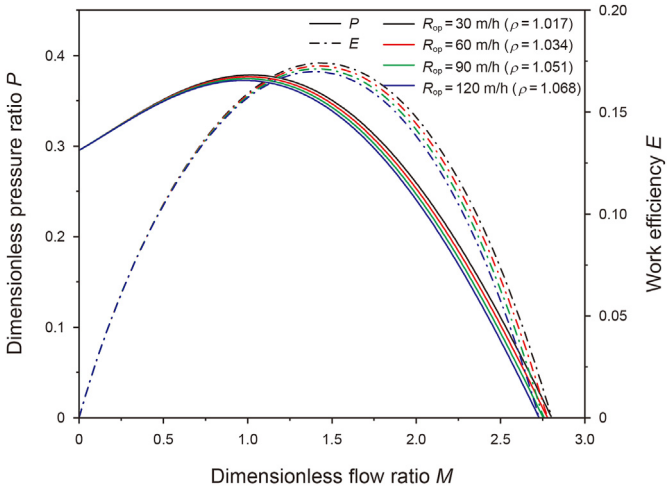

Fig. 11. Hydraulic characteristic curves at different ROP.

From Fig. 11, it can be seen that although the density ratio increases as ROP increases, the increase is very small (the magnitude is 10^{-2}), and the associated decrease in hydraulic depressurization capacity is negligible. It can therefore be considered that the ROP has no effect on the hydraulic depressurization effect of the JMB during drilling.

4. Hydraulic cuttings cleaning modeling of JMB

Besides the hydraulic depressurization capacity, the hydraulic cuttings cleaning capacity is also essential to the JMB performance. In this section, a hydraulic cuttings cleaning model is developed to analyze and optimize the hydraulic cuttings cleaning capacity of JMB.

4.1. Jet hydraulic power of JMB

The jet hydraulic power of a common bit is defined as the drilling fluid hydraulic power lost at the bit during circulation of the drilling fluid (Lim and Chukwu, 1996). The greater the jet hydraulic power, the better the cuttings cleaning effect of the bit. The jet hydraulic power of the bit is written as (Guan et al., 2021)

$$P_b = P_s - P_g - P_{st} - P_a = P_s - K_L Q^{2.8} \tag{36}$$

where P_b is the jet hydraulic power of the bit, kW; P_s is the output power of the mud pump, kW; P_g is the drilling fluid power dissipated at the ground manifold, kW; P_{st} is the drilling fluid power dissipated at the drill string, kW; P_a is the drilling fluid power dissipated in the annulus, kW; K_L is the pressure loss coefficient of the drilling fluid circulation system; and Q is the volume flow of the drilling fluid, L/s.

Because the drilling fluid entering the JMB is split to flow through the forward nozzles and backward nozzles, the hydraulic power of the JMB used to clean cuttings is part of P_b and can be written as

$$P_{bd} = \frac{q_2}{Q} P_b = \frac{q_2}{Q}\left(P_s - K_L Q^{2.8}\right) \tag{37}$$

$$Q = q_1 + q_2 \tag{38}$$

where P_{bd} is the hydraulic power of the JMB used to clean cuttings, kW; q_1 is the volume flow of drilling fluid flowing through backward nozzles, L/s; and q_2 is the volume flow of drilling fluid flowing through forward nozzles, L/s.

Because of the working characteristics of the mud pump, there are two working states according to the different drilling fluid flows, and the power of the mud pump can be written as

$$P_s = \begin{cases} p_r Q, Q < Q_r \\ P_r, Q \geq Q_r \end{cases} \tag{39}$$

where p_r is the rated pressure of the mud pump, MPa; P_r is the rated power of the mud pump, kW; and Q_r is the rated flow of the mud pump, L/s.

Substituting Eqs. (2) and (39) into Eq. (37), the following equation can be obtained:

$$P_{bd} = \begin{cases} \dfrac{M}{1+M}\left(p_r Q - K_L Q^{2.8}\right), Q < Q_r \\ \dfrac{M}{1+M}\left(P_r - K_L Q^{2.8}\right), Q \geq Q_r \end{cases} \tag{40}$$

By derivation, the optimal drilling fluid flow corresponding to the maximum hydraulic power of the JMB can be written as

$$Q_{opt} = \min\left(\left(\frac{p_r}{2.8K_L}\right)^{\frac{1}{1.8}}, Q_r\right) \tag{41}$$

Based on Eq. (40), the jet hydraulic power curve of JMB can be formed as shown in Fig. 12, revealing a maximum hydraulic power point. When the drilling fluid flow is lower than Q_{opt}, the increase in output power of the mud pump exceeds the increase in power loss during drilling fluid circulation, resulting in an increase in jet hydraulic power. When the drilling fluid flow exceeds Q_{opt}, the increase in power loss during drilling fluid circulation is greater than the increase in output power of the mud pump; hence, the jet hydraulic power decreases.

4.2. Jet impact force of JMB

The jet impact force is defined as the total force of the jet on the action area and is conducive to cleaning the bottom hole and transporting cuttings. The jet impact force of the bit is written as (Guan et al., 2021)

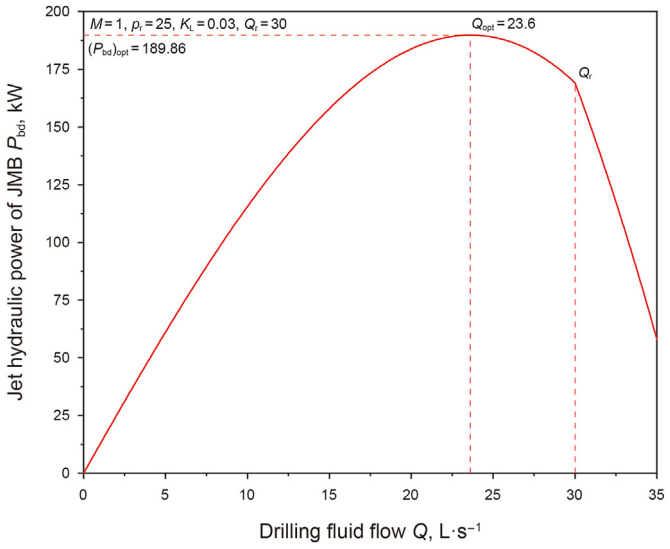

Fig. 12. Jet hydraulic power curve of JMB.

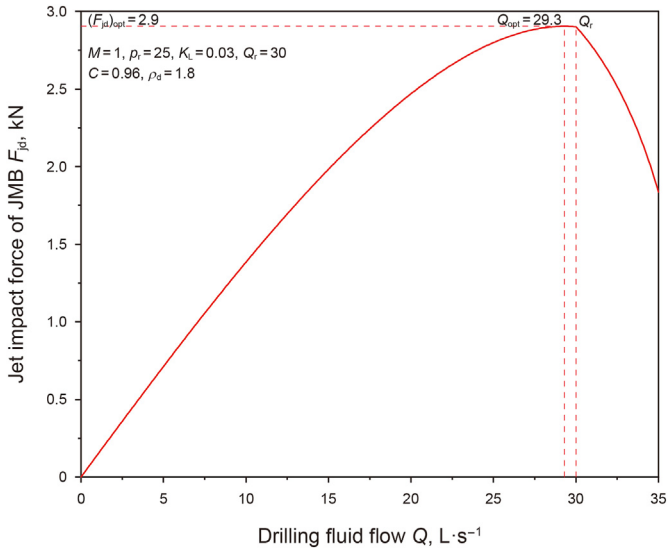

Fig. 13. Jet impact force curve of JMB.

$$F_j = \frac{\rho_d Q v_j}{1000} = \frac{C\sqrt{20\rho_d}}{100} Q\sqrt{p_s - K_L Q^{1.8}} \tag{42}$$

where F_j is the jet impact force of the bit, kN; C is the nozzle flow coefficient; ρ_d is the density of the drilling fluid, g/cm^3; p_s is the output pressure of the mud pump, MPa; and v_j is the jet velocity of the drilling fluid, m/s.

Because the JMB has two kinds of nozzles, the jet impact force determined by Eq. (42) is the sum of the jet impact forces generated by both kinds of nozzles. The following equation can be used to calculate the jet impact force of the JMB:

$$F_{jd} = \frac{Q_{md} v_{jd}}{1000} = \frac{\rho_d q_2 v_j}{1000} \tag{43}$$

where F_{jd} is the jet impact force of the JMB, kN; Q_{md} is the mass flow of the drilling fluid through the forward nozzles, kg/s; and v_{jd} is the velocity of the drilling fluid through the forward nozzles, m/s.

Substituting Eq. (2) into Eq. (43), the following equation can be obtained:

$$F_{jd} = \frac{M}{1+M}\frac{\rho_d Q v_j}{1000} = \frac{M}{1+M}F_j = \frac{M}{1+M}\frac{C\sqrt{20\rho_d}}{100} Q\sqrt{p_s - K_L Q^{1.8}} \tag{44}$$

Considering the working characteristics of mud pumps, Eq. (44) can be rewritten as follows:

$$F_{jd} = \begin{cases} \dfrac{M}{1+M}\dfrac{C\sqrt{20\rho_d}}{100}\sqrt{p_r Q^2 - K_L Q^{3.8}}, Q < Q_r \\ \dfrac{M}{1+M}\dfrac{C\sqrt{20\rho_d}}{100}\sqrt{P_r Q - K_L Q^{3.8}}, Q \geq Q_r \end{cases} \tag{45}$$

By derivation, the optimal drilling fluid flow that corresponds to the maximum jet impact force of the JMB can be written as

$$Q_{opt} = \min\left(\left(\frac{p_r}{1.9K_L}\right)^{\frac{1}{1.8}}, Q_r\right) \tag{46}$$

Based on Eq. (45), the jet impact force curve of the JMB can be represented by Fig. 13, which has the same changing rules as Fig. 12.

4.3. Parametric study of hydraulic cuttings cleaning capacity of JMB

Based on Eqs. (40) and (45), the hydraulic power and jet impact power of the JMB can be described by the following functional forms:

$$P_{bd} = f_{bd}(M, p_r, K_L, Q) \tag{47}$$

$$F_{jd} = f_{jd}(M, C, \rho_d, p_r, K_L, Q) \tag{48}$$

In the actual drilling field, the adjustable parameters in Eqs. (47) and (48) are the flow ratio M, pressure loss coefficient K_L, and the drilling fluid flow Q, where K_L is dependent on the depth of the well. In light of this, the effects of the flow ratio and well depth on the hydraulic power and jet impact power of the JMB are investigated in this section.

4.3.1. Effect of flow ratio

Based on Eqs. (40) and (45), Figs. 14 and 15 can be generated. It can be observed that the hydraulic cuttings cleaning capacity

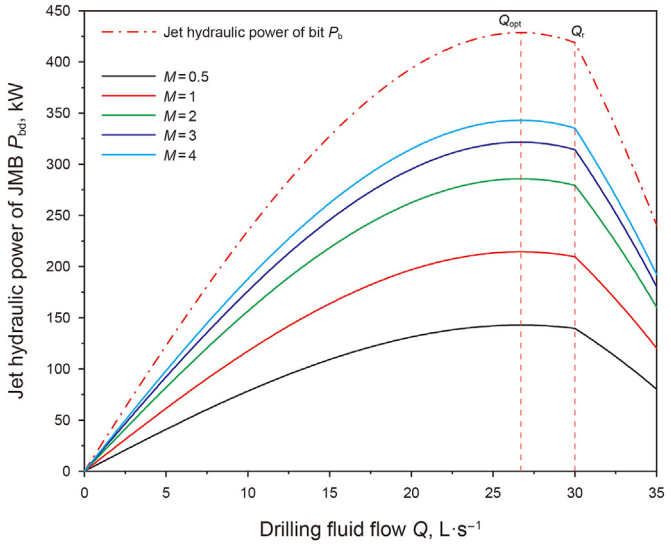

Fig. 14. Jet hydraulic power curves of JMB with different flow ratios M.

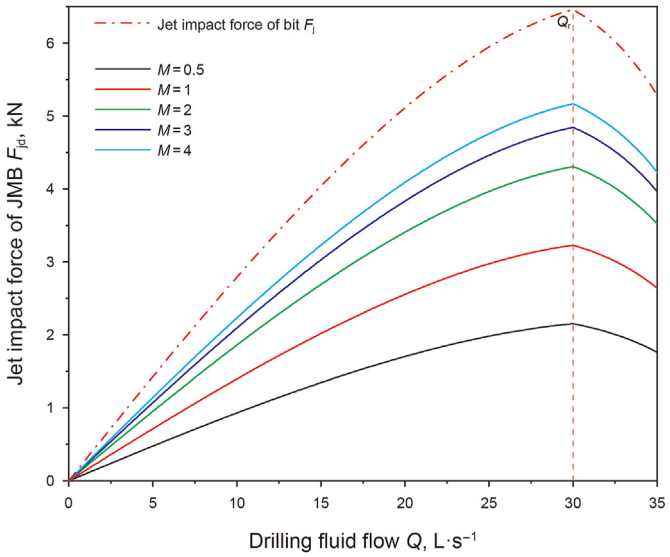

Fig. 15. Jet impact force curves of JMB with different flow ratios M.

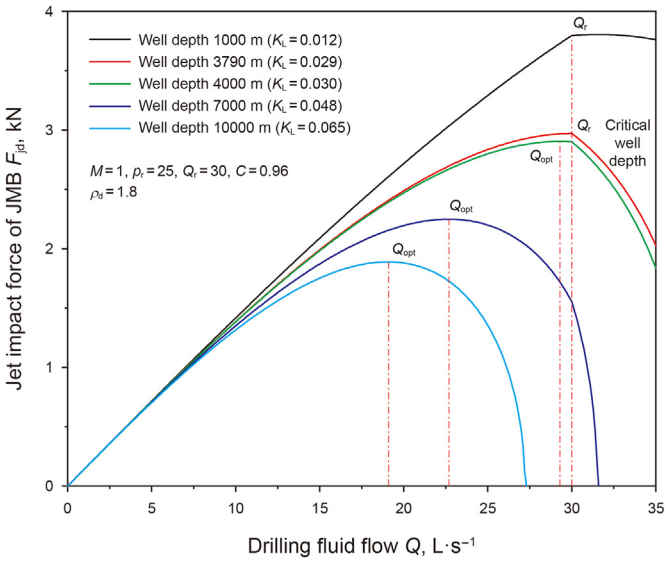

Fig. 17. Jet impact force curves of JMB at different well depths.

decrease as the flow ratio M decreases since a decrease in M indicates a decrease in drilling fluid flow through the forward nozzles. M only affects the value of hydraulic cuttings cleaning capacity but not the optimal drilling fluid flow.

4.3.2. Effect of well depth

K_L can be written as

$$K_L = \alpha D + \beta \tag{49}$$

where D is the well depth, m; and α and β are the specific coefficients, which can be determined based on drilling conditions.

Based on Eqs. (40) and (45), Figs. 16 and 17 are obtained for different well depths. As the depth increases, the hydraulic loss increases, and the hydraulic cuttings cleaning capacity decrease. In addition, because of the constraint of the mud pump's rated flow Q_r, the optimal drilling fluid flow cannot exceed Q_r.

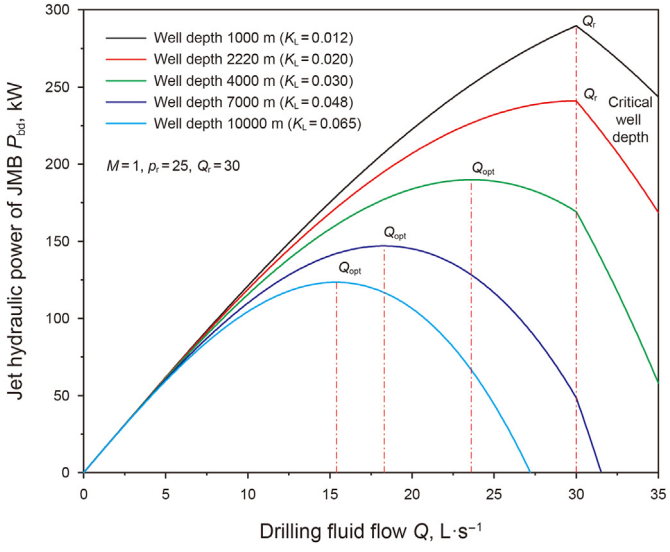

Fig. 16. Jet hydraulic power curves of JMB at different well depths.

5. Hydraulic optimization of JMB

The JMB has two types of hydraulic capacities: hydraulic depressurization capacity and hydraulic cuttings cleaning capacity. The objective of the hydraulic optimization of a JMB is to maximize the overall performance of the JMB, which is defined as simultaneously maximizing the hydraulic depressurization capacity and hydraulic cuttings cleaning capacity. By combining two hydraulic models, the optimization objectives can be described as maximizing the working efficiency and jet hydraulic power of the JMB or maximizing the working efficiency and jet impact force of the JMB.

5.1. Objective functions of hydraulic optimization

The working efficiency of the JMB can be written as

$$E = f_E(M, \rho, R, K_{ju}, K_s, K_{td}, \xi) \tag{50}$$

The jet hydraulic power and jet impact force of the JMB can be written as

$$P_{bd} = f_{bd}(M, p_r, K_L, Q) \tag{51}$$

$$F_{jd} = f_{jd}(M, C, \rho_d, p_r, K_L, Q) \tag{52}$$

According to Section 3.4.3, the density ratio ρ has a negligible effect on the working efficiency of the JMB during drilling. The frictional loss coefficients (K_{ju}, K_s, and K_{td}) depend on the surface quality of flow channels, which cannot be adjusted during the design process. The loss coefficient ξ depends on the target inclination angle, which must be determined by striking a balance between JMB hydraulics and secondary cuttings crushing effect. The M and R in Eq. (50) are therefore selected as control parameters for the hydraulic optimization of the JMB.

The objective functions for maximizing the working efficiency and jet hydraulic power of the JMB can be written as

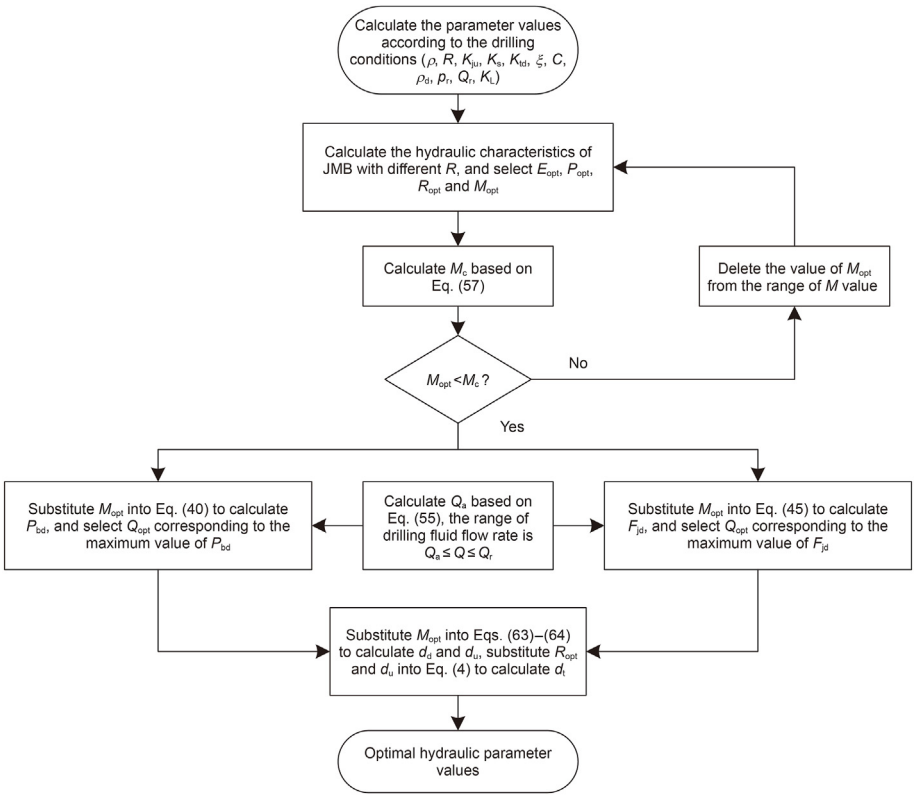

Fig. 18. Process of hydraulic optimization of JMB.

Table 2
Parameters of JMB.

Parameter	Value	Parameter	Value
K_{ju}	0.15	θ	40 deg
K_s	0.2	ρ	1
K_{td}	0.38		

$$\text{obj.}\begin{cases}\max E = f_E(M,R) = \dfrac{M^2 - M\lambda + M}{M^2 + M + \lambda} \\ \max P_{bd} = f_{bd}(M,Q) = \begin{cases}\dfrac{M}{1+M}\left(p_r Q - K_L Q^{2.8}\right), Q < Q_r \\ \dfrac{M}{1+M}\left(P_r - K_L Q^{2.8}\right), Q \ge Q_r\end{cases}\end{cases} \tag{53}$$

The objective functions for maximizing the working efficiency and jet impact force of the JMB can be written as

$$\text{obj.}\begin{cases}\max E = f_E(M,R) = \dfrac{M^2 - M\lambda + M}{M^2 + M + \lambda} \\ \max F_{jd} = f_{jd}(M,Q) = \begin{cases}\dfrac{M}{1+M}\dfrac{C\sqrt{20\rho_d}}{100}\sqrt{p_r Q^2 - K_L Q^{3.8}}, Q < Q_r \\ \dfrac{M}{1+M}\dfrac{C\sqrt{20\rho_d}}{100}\sqrt{P_r Q - K_L Q^{3.8}}, Q \ge Q_r\end{cases}\end{cases} \tag{54}$$

5.2. Constraints of hydraulic optimization

To ensure that cuttings can rise constantly with drilling fluid, the flow of drilling fluid has a constraint of minimum (Altun and Osgouei, 2014; Hemphill and Larsen, 1996; Ozbayoglu et al., 2007), which is written as

$$Q_a = \frac{\pi}{40}\left(d_h^2 - d_p^2\right)v_a \tag{55}$$

$$v_a = \frac{18.24}{\rho_d d_h} \tag{56}$$

where Q_a is the minimal drilling fluid flow required to transport cuttings, L/s; d_h is the diameter of the wellbore, cm; d_p is the diameter of the cuttings particle, m; and v_a is the minimum annulus velocity, m/s.

The excessive flow rate of drilling fluid through the annulus of the throat may result in a cavitation effect (Gohil and Saini, 2014; Shervani-Tabar et al., 2012), which is detrimental to the hydraulic performance and structural integrity of the JMB. Cavitation develops when the flow ratio exceeds the maximum flow ratio (Kudirka and DeCoster, 1979), which is written as

$$M_c = \frac{1-R}{R}\sqrt{\frac{p_3}{I_c(p_1 - p_3) + p_3}} = \frac{1-R}{R}\sqrt{\frac{p_{31}}{I_c(1 - p_{31}) + p_{31}}} \tag{57}$$

$$p_{31} = \frac{p_3}{p_1} \tag{58}$$

where M_c is the maximum allowed flow ratio before cavitation occurs; and I_c is the empirical coefficient of cavitation, whose value is typically 1.35.

Table 3
Drilling parameters.

Parameter	Value	Parameter	Value
Density of drilling fluid ρ_d	1.8 g/cm^3	Plastic viscosity of drilling fluid μ_{pv}	0.1 Pa s
Diameter of borehole d_h	21.6 cm	Inner diameter of drill pipe d_{pi}	10.86 cm
Outer diameter of drill pipe d_{po}	12.7 cm	Constant B	0.51655
Inner diameter of drill collar d_{ci}	7.14 cm	Outer diameter of drill collar d_c	17.78 cm
Length of drill collar L_c	100 m	Nozzle flow coefficient C	0.96
Length of high-pressure pipeline L_1	451 m	Inner diameter of high-pressure pipeline d_1	11.2 cm
Length of riser L_2	10 m	Inner diameter of riser d_2	13 cm
Length of hose L_3	12 m	Inner diameter of hose d_3	13 cm
Length of kelly pipe L_4	18 m	Inner diameter of kelly pipe d_4	12 cm
Rated pressure of mud pump p_r	20 MPa	Rated flow of mud pump Q_r	40 L/s

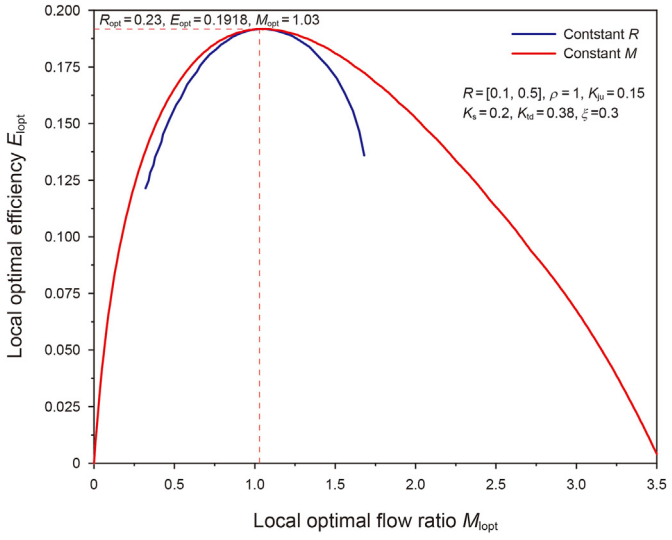

Fig. 19. Curves of local optimal efficiency.

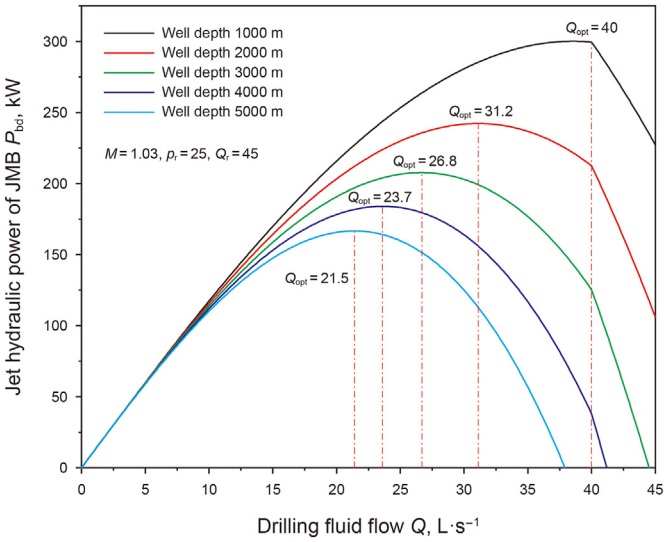

Fig. 21. Curves of jet hydraulic power of JMB at different well depths.

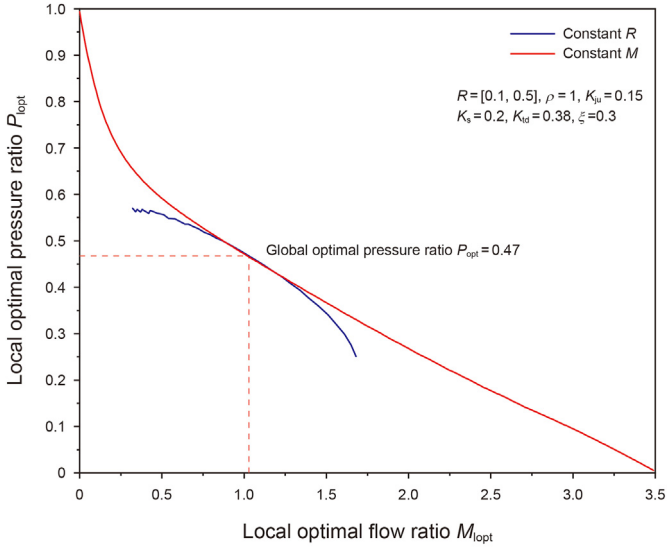

Fig. 20. Curves of local optimal pressure ratio.

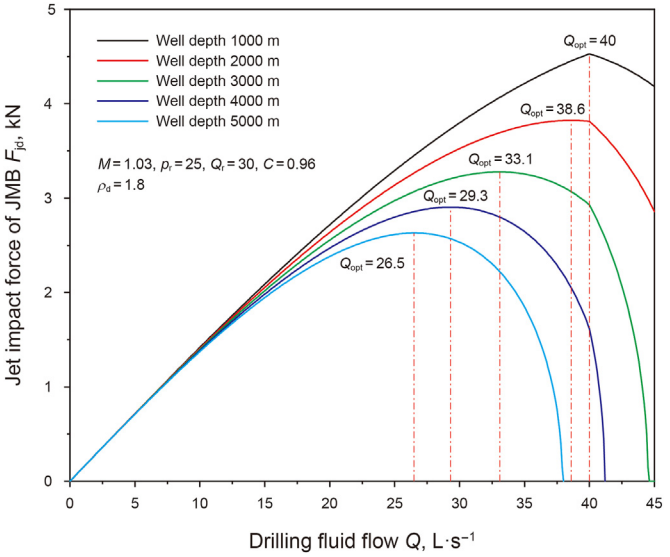

Fig. 22. Curves of jet impact force of JMB at different well depths.

Table 4
Optimal hydraulic parameters of JMB (maximizing working efficiency and jet hydraulic power).

Parameter	Parameter value				
Global optimal area ratio R_{opt}	0.23				
Global optimal flow ratio M_{opt}	1.03				
Global optimal efficiency E_{opt}	0.1918				
Global optimal pressure ratio P_{opt}	0.47				
Well depth, km	1	2	3	4	5
Optimal drilling fluid flow Q_{opt}, L/s	40	31.2	26.8	23.7	21.5
Optimal jet hydraulic power of JMB P_{bd}, kW	313.62	253.63	217.36	192.67	174.50
Diameter of backward nozzle d_u, mm	7.30	6.31	5.85	5.49	5.23
Diameter of forward nozzle d_d, mm	7.41	6.40	5.94	5.57	5.31
Diameter of throat d_t, mm	15.23	13.15	12.20	11.45	10.91

Table 5
Optimal hydraulic parameters of JMB (maximizing working efficiency and jet impact force).

Parameter	Parameter value				
Global optimal area ratio R_{opt}	0.23				
Global optimal flow ratio M_{opt}	1.03				
Global optimal efficiency E_{opt}	0.1918				
Global optimal pressure ratio P_{opt}	0.47				
Well depth, km	1	2	3	4	5
Optimal drilling fluid flow Q_{opt}, L/s	40	38.6	33.1	29.3	26.5
Optimal jet impact force of JMB F_{jd}, kN	4.60	3.88	3.33	2.95	2.67
Diameter of backward nozzle d_u, mm	7.30	8.52	7.90	7.42	7.04
Diameter of forward nozzle d_d, mm	7.41	8.65	8.02	7.53	7.14
Diameter of throat d_t, mm	15.23	17.77	16.47	15.47	14.68

In summary, the constraints of the hydraulic optimization of the JMB can be written as

$$\text{s.t.}\begin{cases} Q \geq Q_a \\ M \leq M_c \end{cases} \tag{59}$$

5.3. Process of hydraulic optimization of JMB

The equivalent diameter of nozzles can be written as (Guan et al., 2021)

$$d_{ne} = \sqrt{\sum_{i=1}^{n_1} (d_u)_i^{\,2} + \sum_{i=1}^{n_2} (d_d)_i^{\,2}} \tag{60}$$

$$d_{ne} = \sqrt[4]{\frac{0.081\rho_d Q_{opt}^2}{C^2 \Delta p_b}} = \sqrt[4]{\frac{0.081\rho_d Q_{opt}^2}{C^2\left(p_r - K_L Q_{opt}^{1.8}\right)}} \tag{61}$$

By considering that the JMB has two types of nozzles, Eq. (60) can be written as

$$\sum_{i=1}^{n_1} (d_u)_i^{\,2} + M\sum_{i=1}^{n_2} (d_u)_i^{\,2} = \sqrt{\frac{0.081\rho_d Q_{opt}^2}{C^2\left(p_r - K_L Q_{opt}^{1.8}\right)}} \tag{62}$$

where n_1 is the number of backward nozzles, and n_2 is the number of forward nozzles.

When the number of forward and backward nozzles is equal, the diameter of the nozzles can be calculated by the following equations:

$$d_u = \frac{\sqrt[4]{\frac{0.081\rho_d Q_{opt}^2}{C^2\left(p_r - K_L Q_{opt}^{1.8}\right)}}}{\sqrt{n_1(1+M)}} \tag{63}$$

$$d_d = \sqrt{M}\,\frac{\sqrt[4]{\frac{0.081\rho_d Q_{opt}^2}{C^2\left(p_r - K_L Q_{opt}^{1.8}\right)}}}{\sqrt{n_1(1+M)}} \tag{64}$$

The hydraulic optimization process of the JMB is shown in Fig. 18.

5.4. Case study

In this section, drilling field data are utilized for the hydraulic optimization of the JMB. The JMB parameters are listed in Table 2.

Well Jiaoye31-S1HF is a shale gas well with a long horizontal interval in Chongqing, China. This well has the problem of low ROP because of hard formation and cuttings bed, and the JMB is expected to address these problems. The drilling parameters of the Jiaoye31-S1HF well are listed in Table 3 and are used to optimize the hydraulics of the JMB.

Based on Eqs. (32) and (33), by using the parameter values in Table 2, the hydraulic depressurization parameters of the JMB are calculated and shown in Figs. 19 and 20. The global optimal pressure ratio R_{opt} is 0.23, the global optimal flow ratio M_{opt} is 1.03, the global optimal efficiency E_{opt} is 0.1918, and the global optimal pressure ratio P_{opt} is 0.47.

Assuming that the maximum range of p_{31} is (0.6, 1), when p_{31} is substituted into Eq. (57), the maximum range of M_c is (2.17, 3), which is plainly bigger than the global optimal pressure ratio M_{opt} (1.03). Thus, the aforementioned optimization results are appropriate.

By substituting M_{opt} into Eqs. (40) and (45), the curves of the jet hydraulic power and jet impact force of the JMB can be obtained as depicted in Figs. 21 and 22, as well as the corresponding Q_{opt}.

According to Eqs. (55) and (56), the minimum drilling fluid can be calculated as

$$v_a = \frac{18.24}{1.8 \times 21.6} = 0.47 \text{ m/s} \tag{65}$$

$$Q_a = 11.27 \text{ L/s} \tag{66}$$

The optimal drilling fluid flows at different well depths are bigger than the minimal drilling fluid Q_a, which meets the drilling fluid flow limitation, as indicated in Eq. (59).

Moreover, by substituting Q_{opt} into Eqs. (63) and (64), the sizes of the forward and backward nozzles can be determined. The optimal hydraulic parameters of the JMB can be obtained according to the hydraulic optimization method, as shown in Tables 4 and 5.

6. Conclusions

In this paper, the hydraulics of the JMB were studied by considering the characteristics of depressurization and cuttings cleaning. Good performance of the JMB is not inseparable from good hydraulic depressurization capacity and good hydraulic cuttings cleaning capacity. Therefore, the hydraulics of the JMB require a comprehensive analysis of these two hydraulic capacities.

A hydraulic depressurization model of the JMB was developed based on jet pump theory, and the pressure ratio and efficiency were chosen as the evaluation parameters of the depressurization capacity. Parametric study results showed that an increase in the friction loss coefficients and target inclination angle causes a significant reduction in the hydraulic depressurization capacity, and the effect of ROP is negligible. The optimal area ratio and optimal flow ratio can be determined by hydraulic characteristic curves that are drawn based on the hydraulic depressurization model.

A hydraulic cuttings cleaning model of the JMB was developed based on the theories of jet hydraulic power and jet impact force. Parametric study results showed that the flow ratio is positively related to the hydraulic cuttings cleaning capacity, and the well depth determines the maximum hydraulic cuttings cleaning capacity. The optimal drilling fluid flow corresponding to the maximum cuttings cleaning capacity can be calculated according to the given methods.

By combining the hydraulic depressurization model and hydraulic cuttings cleaning model, an optimization method of JMB hydraulics was proposed to simultaneously maximize the depressurization capacity and cuttings cleaning capacity. According to the given optimization procedure, the optimal values of the drilling fluid flow, backward nozzle diameter, forward nozzle diameter, and throat diameter can be calculated. The above work will provide guidance for the optimization and application of the JMB.

Declaration of competing interest

The authors declare that they have no known competing financial interests or personal relationships that could have appeared to influence the work reported in this paper.

Acknowledgement

This work was financially supported by Youth Project of Natural Science Basic Research Program of Shaanxi Province (Grant number: 2023-JC-QN-0538); Scientifical Research Program for Youth Innovation Team Construction of Shaanxi Provincial Department of Education (Grant number: 21JP054, 22JP032); National Natural Science Foundation of China (Grant numbers: 52174012; 51804322; 51821092; 51774301; U1762214), and Open Fund (PLC 20210404) of State Key Laboratory of Oil and Gas Reservoir Geology and Exploitation (Chengdu University of Technology)

References

Adesina, F.A., Churchill, A., Olugbenga, F., 2011. Modeling productivity index for long horizontal well. J. Energy Resour. Technol. 133 (3), 33–101. https://doi.org/10.1115/1.4004887.

Altun, G., Osgouei, A.E., 2014. Investigation and remediation of active-clay contaminated sepiolite drilling muds. Appl. Clay Sci. 102, 238–245. https://doi.org/10.1016/j.clay.2014.10.002.

Beithou, N., Aybar, H.S., 2001. High-pressure steam-driven jet pump—Part I: mathematical modeling. J. Eng. Gas Turbines Power 123 (3), 693–700. https://doi.org/10.1115/1.1365934.

Berger, S.A., Talbot, L., Yao, L.S., 1983. Flow in curved pipes. Annu. Rev. Fluid Mech. 15 (1), 461–512. https://doi.org/10.1146/annurev.fl.15.010183.002333.

Cao, T., Yu, K., Chen, X., et al., 2019. Numerical and experimental investigation on the feasibility of horizontal drilling with a new type of jet mill bit. J. Energy Resour. Technol. 141 (9), 93–101. https://doi.org/10.1115/1.4043246.

Chen, X., Gao, D., 2016. Jet mill bit for improving cuttings carrying capacity in horizontal gas drilling. Abu Dhabi International Petroleum Exhibition & Conference. Soc. Petroleum Eng. https://doi.org/10.2118/183032-MS.

Chen, X., Gao, D., Guo, B., 2016a. A method for optimizing jet-mill-bit hydraulics in horizontal drilling. SPE J. 21 (2), 416–422. https://doi.org/10.1016/j.jngse.2015.12.033.

Chen, X., Gao, D., Guo, B., 2016b. Optimal design of jet mill bit for jet comminuting cuttings in horizontal gas drilling hard formations. J. Nat. Gas Sci. Eng. 28, 587–593. https://doi.org/10.1016/j.jngse.2015.12.033.

Chen, X., Cao, T., Yu, K., et al., 2020. Numerical and experimental investigation on the depressurization capacity of a new type of depressure-dominated jet mill bit. Petrol. Sci. 2020 (17), 1602–1615. https://doi.org/10.1007/s12182-020-00472-8.

Chen, P., Miska, S., Yu, M., et al., 2021a. Modeling of cutting rock: from PDC cutter to PDC bit—modeling of PDC bit. SPE J. 26 (6), 3465–3487. https://doi.org/10.2118/206725-PA.

Chen, P., Miska, S., Yu, M., et al., 2021b. Modeling of cutting rock: from PDC cutter to PDC bit—modeling of PDC cutter. SPE J. 26 (6), 3444–3464. https://doi.org/10.2118/205342-PA.

Cunningham, R., 1957. Jet-pump theory and performance with fluids of high viscosity. Trans. Am. Soc. Mech. Eng. 79 (8), 1807–1819. https://doi.org/10.1115/1.4013500.

Gohil, P.P., Saini, R., 2014. Coalesced effect of cavitation and silt erosion in hydro turbines—a review. Renew. Sustain. Energy Rev. 33, 280–289. https://doi.org/10.1016/j.rser.2014.01.075.

Gosline, J.E., O'Brien, J.P., 1934. The water jet pump. Univ. Calif. Publ. Entomol. 3, 167–190. https://agris.fao.org/agris-search/search.do?recordID=US201300637573.

Grupping, A., Coppes, J., Groot, J., 1988. Fundamentals of oilwell jet pumping. SPE Prod. Eng. 3 (1), 9–14. https://doi.org/10.2118/15670-PA.

Guan, Z., Chen, T., Liao, H., 2021. Theory and Technology of Drilling Engineering. Springer Singapore, Singapore. https://doi.org/10.1007/978-981-15-9327-7.

Hemphill, T., Larsen, T., 1996. Hole-cleaning capabilities of water-and oil-based drilling fluids: a comparative experimental study. SPE Drill. Complet. 11 (4), 201–207. https://doi.org/10.2118/26328-PA.

Kendall, H., Goins, W., 1960. Design and operation of jet-bit programs for maximum hydraulic horsepower, impact force or jet velocity. Transact. AIME 219 (1), 238–250. https://doi.org/10.2118/1288-G.

Kermit, E.B., 1980. The technology of artificial lift methods. Petroleum Publishing 1 (2).

Kudirka, A.A., DeCoster, M.A., 1979. Jet pump cavitation with ambient and high temperature water. J. Fluid Eng. 101 (1), 93–99. https://doi.org/10.1115/1.3448741.

Lim, K.M., Chukwu, G.A., 1996. Bit hydraulics analysis for efficient hole cleaning. SPE Western Regional Meeting. Soc. Petroleum Eng. https://doi.org/10.2118/35667-MS. Anchorage, Alaska.

Liu, X., Tang, P., Geng, Q., et al., 2019. Effect of abrasive concentration on impact performance of abrasive water jet crushing concrete. Shock Vib. 2019, 3285150. https://doi.org/10.1155/2019/3285150.

McLean, R., 1965. Velocities, kinetic energy and shear in crossflow under three-cone jet bits. J. Petrol. Technol. 17 (12), 1443–1448. https://doi.org/10.2118/1306-PA.

Ozbayoglu, M.E., Saasen, A., Sorgun, M., et al., 2007. Estimating critical velocity to prevent bed development for horizontal-inclined wellbores. SPE/IADC Middle East Drilling and Technology Conference. Soc. Petroleum Eng. https://doi.org/10.2118/108005-MS. Cairo, Egypt.

Qi, Q., 2017. Engineering Fluid Mechanics. Tsinghua University Press, China. http://www.tup.tsinghua.edu.cn/booksCenter/book_06554701.html (in Chinese).

Rankine, W.J.M., 1871. On the mathematical theory of combined streams. Proc. Roy. Soc. Lond. 19 (123–129), 90–94. https://doi.org/10.1098/rspl.1870.0018.

Schnuriger, M., Cuillier, B., Tilleman, D., et al., 2017. Curved nozzle design for PDC bits enhances hydraulics for bit cleaning and cooling improvements. SPE/IADC Drilling Conference and Exhibition. Soc. Petroleum Eng. The Hague, The Netherlands. https://doi.org/10.2118/184734-MS.

Shervani-Tabar, M.T., Parsa, S., Ghorbani, M., 2012. Numerical study on the effect of the cavitation phenomenon on the characteristics of fuel spray. Math. Comput. Model. 56 (5–6), 105–117. https://doi.org/10.1016/j.mcm.2011.12.012.

Speer, J.W., 1959. A method for determining optimum drilling techniques. In: Gulf Coast Drilling and Production Meeting. OnePetro. https://doi.org/10.2118/1242-G.

Tang, H., Sun, Z., He, Y., et al., 2019. Investigating the pressure characteristics and production performance of liquid-loaded horizontal wells in unconventional gas reservoirs. J. Petrol. Sci. Eng. 176, 456–465. https://doi.org/10.1016/j.petrol.2019.01.072.

Wang, C., Lin, J., Lin, J., 2004a. Research on energy distribution and efficiency characteristics of jet pump systems. China Mech. Eng. 15 (4), 297–300. https://kns.cnki.net/kcms2/article/abstract?v=3uoqIhG8C44YLTlOAiTRKgchrJ08w1e7eeyE9jLkqq_oyRDrdsw-vb1PMGnXV0lHbJkFw4KhJS0FeCb2-iLf8rD6YEam7G5z&uniplatform=NZKPT (in Chinese).

Wang, C., Lin, J., Shi, X., 2004b. Method of optimal parameter ascertainment of jet pump. Fluid Mach. 32 (9), 21–25. https://kns.cnki.net/kcms2/article/abstract?v=3uoqIhG8C44YLTlOAiTRKgchrJ08w1e7eeyE9jLkqq9hQsr5meJfkryh5PQlwb-4-vAK0PJ2fR8oR4HrYCRC8vPRjsjM1zxF&uniplatform=NZKPT (in Chinese).

Wang, G., Wang, Y., Yang, X., et al., 2021. Gas jet coal-breaking behavior: an elliptical

crushing theoretical model. Geofluids 2021, 4300088. https://doi.org/10.1155/2021/4300088.
Wells, M., Marvel, T., Beuershausen, C., 2008. Bit balling mitigation in PDC bit design. In: IADC/SPE Asia Pacific drilling technology conference and exhibition. OnePetro. https://doi.org/10.2118/114673-MS.
Winoto, S., Li, H., Shah, D., 2000. Efficiency of jet pumps. J. Hydraul. Eng. 126 (2), 150–156. https://doi.org/10.1061/(ASCE)0733-9429.
Wu, Z., Deng, S., He, X., et al., 2020. Numerical simulation and dimension reduction analysis of electromagnetic logging while drilling of horizontal wells in complex structures. Petrol. Sci. 17 (3), 645–657. https://doi.org/10.1007/s12182-020-00444-y.
Zhu, H., Liu, Q., 2015. Pressure drawdown mechanism and design principle of jet pump bit. Sci. Iran. 22 (3), 792–803. http://scientiairanica.sharif.edu/article_3672.html.